Stable, mobile, dark-in-bright, dipolar Bose-Einstein-condensate solitons

S. K. Adhikari*

Instituto de Física Teórica, Universidade Estadual Paulista, 01.140-070 São Paulo, São Paulo, Brazil

(Received 22 January 2014; revised manuscript received 8 April 2014; published 23 April 2014)

We demonstrate robust, stable, mobile, quasi-one-dimensional, dark-in-bright dipolar Bose-Einstein-condensate (BEC) solitons with a notch in the central plane formed due to dipolar interaction for repulsive contact interaction. At medium velocity the head-on collision of two such solitons is found to be quasielastic with practically no deformation. A proposal for creating dipolar dark-in-bright solitons in laboratories by phase imprinting is also discussed. A rich variety of such solitons can be formed in dipolar binary BECs, where one can have a dark-in-bright soliton coupled to a bright soliton or two coupled dark-in-bright solitons. The findings are illustrated using numerical simulation in three spatial dimensions by employing realistic interaction parameters for a dipolar ^{164}Dy BEC and a binary ^{164}Dy-^{162}Dy BEC.

DOI: 10.1103/PhysRevA.89.043615 PACS number(s): 03.75.Hh, 03.75.Mn, 03.75.Kk, 03.75.Lm

I. INTRODUCTION

A bright soliton is a self-reinforcing solitary wave in the form of a local peak in density that maintains its shape, while traveling at a constant velocity in one dimension, due to a cancellation of nonlinear attraction and dispersive effects. A dark soliton corresponds to a dip in uniform density in one dimension, which also can move with a constant velocity maintaining its shape. Solitons have been studied in water waves, nonlinear optics, Bose-Einstein condensates (BEC), etc. [1]. In the physical three-dimensional (3D) world, quasisolitons are observed where a reduced (integrated) one-dimensional (1D) density exhibits solitonlike properties. Experimentally, bright matter-wave solitons and soliton trains were created in a BEC of ^{7}Li [2] and ^{85}Rb atoms [3] by turning the atomic interaction attractive from repulsive using a Feshbach resonance [4] and releasing the BEC in an axially free or an expulsive trap [5]. However, due to collapse instability, in three dimensions, bright solitons are fragile and can accommodate only a small number of atoms.

A dark soliton corresponds to a notch (zero) in a uniform 1D density, which can propagate with a constant velocity. However, this condition cannot be realized in a trapped 3D BEC, where a notch in a plane passing through the center has been termed a dark soliton. Such a dark soliton in a trapped BEC has been observed experimentally and its small (axial) oscillation around the center has been studied [6–8]. However, the long-time dynamics of BEC dark solitons has always been found to be unstable [8–10], except for a very strong transverse trapping condition leading to a quasi-1D situation. For moderate to weak transverse traps, both theoretical and experimental considerations reveal that these dark solitons in BECs are unstable, exhibit snake instability [8], and eventually decay, forming a vortex ring [11]. In addition, the trapped dark solitons can decay by a slow viscous acceleration due to their negative effective mass [9]. Although, experimentally realizable, dark solitons in a trapped BEC can hardly be termed a soliton, as neither the notch nor the trapped BEC can move with a constant velocity without a change of shape as in the case of an integrable 1D dark or bright soliton. Moreover, the dark solitons of a trapped BEC are realized in a fully repulsive setup and the trap in the axial direction cannot be removed, as in a bright soliton, to make the dark soliton mobile in the axial direction.

The recent study of BECs of ^{164}Dy [12,13], ^{168}Er [14], and ^{52}Cr [15,16] atoms with large magnetic dipole moments has initiated new investigations of BEC solitons in a different scenario. It is possible to have dipolar BEC solitons for a fully repulsive contact interaction [17]. The dipolar BEC solitons of a large number of atoms, stabilized by long-range dipolar attraction, could be robust and less vulnerable to collapse in three dimensions due to the short-range contact repulsion. Quasi-1D [17], quasi-two-dimensional (2D) [18], vortex [19], and dark [20] solitons have been predicted in dipolar BECs. Dipolar BEC solitons can also be stabilized in periodic optical-lattice traps by replacing the usual harmonic traps in quasi-1D [21] and quasi-2D [19] setups.

Taking advantage of the robust nature of the large dipolar bright solitons, we consider a different class of bright solitons with a notch in the central radial plane and capable of moving in the axial direction with a constant velocity without deformation. We call these objects dark-in-bright solitons, which are stretched in the axial direction compared to the bright soliton without a notch. They are stable and stationary excitations of the bright soliton. The head-on collision between two dark-in-bright solitons or between a dark-in-bright and a bright soliton is found to be quasielastic at medium velocities of a few mm/s. In such a collision, two solitons pass through each other without significant deformation. However, as the velocity is further lowered, the collision becomes inelastic with visible deformation of the solitons during collision. The collision of solitons can be completely elastic only in 1D integrable systems.

We also consider the possibility of the creation of the dark-in-bright solitons without axial trapping by phase imprinting [6,22] over a normal bright soliton with identical parameters. We consider the dynamical evolution of a bright soliton where the two halves have opposite phases. Upon dynamical numerical simulation such a soliton is found to develop a notch in the central radial plane between the two halves with opposite phases as in a dark soliton [8]. As the

*adhikari@ift.unesp.br; http://www.ift.unesp.br/users/adhikari

present dark-in-bright solitons are realized in the absence of axial trapping, unlike the conventional dark solitons of a trapped BEC, these are capable of moving with a constant velocity. Such dark-in-bright solitons formed due to the long-range dipolar interaction are not realizable in nondipolar BECs.

These axially free dark-in-bright solitons are so robust that they can also be realized in binary dipolar BECs. In binary BECs two stable configurations were considered: (i) one distinct dark-in-bright soliton in each component and (ii) a dark-in-bright soliton in one component coupled to a bright soliton in the other component.

In Sec. II the time-dependent 3D mean-field model for the binary dipolar BEC soliton is presented. The results of numerical calculation are exhibited in Sec. III. The domain of a stable bright and dark-in-bright solitons is illustrated in a stability phase diagram showing the maximum number of ^{164}Dy and ^{168}Er atoms versus the respective scattering lengths. The dynamical evolution of the collision between two dark-in-bright solitons and between a bright and a dark-in-bright soliton is considered. The evolution of a phase-imprinted bright soliton to a dark-in-bright soliton is also demonstrated. The stability phase diagram for the appearance of dark-in-bright solitons in the binary ^{164}Dy-^{162}Dy mixture is also considered. Finally, in Sec. IV a brief summary of our findings is presented.

II. MEAN-FIELD MODEL

The extension of the mean-field Gross-Pitaevskii (GP) equation to binary dipolar boson-boson [23] and boson-fermion [24] mixtures is well established and for the sake of completeness we give a brief summary of the same appropriate for this study. We present the binary GP equations in dimensionless form, which is more practical to use and has a neater look.

A. Binary BEC

We consider a binary dipolar BEC soliton, with the mass, number of atoms, magnetic dipole moment, and scattering length for the two species $j = 1,2$ given by m_j, N_j, μ_j, and a_j, respectively. The intraspecies V_j and interspecies V_{12} interactions for two atoms at $\mathbf{r}$ and $\mathbf{r}'$ are

$$V_j(\mathbf{R}) = 3a_{\rm dd}^{(j)} V_{\rm dd}(\mathbf{R}) + 4\pi a_j \delta(\mathbf{R}), \tag{1}$$

$$V_{12}(\mathbf{R}) = 3a_{\rm dd}^{(12)} V_{\rm dd}(\mathbf{R})/2 + 2\pi a_{12} \delta(\mathbf{R}), \tag{2}$$

respectively, with

$$a_{\rm dd}^{(j)} = \frac{\mu_0 \mu_j^2 m_j}{12\pi\hbar^2}, \qquad a_{\rm dd}^{(12)} = \frac{\mu_0 \mu_1 \mu_2 m_1 m_2}{6\pi\hbar^2 (m_1+m_2)}, \tag{3}$$

$$V_{\rm dd}(\mathbf{R}) = \frac{1-3\cos^2\theta}{\mathbf{R}^3}, \tag{4}$$

where a_{12} is the intraspecies scattering length, μ_0 is the permeability of free space, θ is the angle made by the vector $\mathbf{R}$ with the polarization z direction, and $\mathbf{R} = (\mathbf{r} - \mathbf{r}')$. The strengths of intraspecies and interspecies dipolar interactions are here expressed in terms of the dipolar lengths $a_{\rm dd}^{(j)}$ and $a_{\rm dd}^{(12)}$ given by Eq. (3) in the same way that the strengths of contact interactions are expressed in terms of scattering lengths a_j and a_{12}. The dimensionless GP equations for the axially free quasi-1D binary soliton can be written as [23]

$$i\frac{\partial\phi_1(\mathbf{r},t)}{\partial t} = \Big[-\frac{\nabla^2}{2} + \frac{1}{2}\rho^2 + g_1|\phi_1|^2 + g_{12}|\phi_2|^2 + g_{\rm dd}^{(1)} \int V_{\rm dd}(\mathbf{R})|\phi_1(\mathbf{r}',t)|^2 d\mathbf{r}' + g_{\rm dd}^{(12)} \int V_{\rm dd}(\mathbf{R})|\phi_2(\mathbf{r}',t)|^2 d\mathbf{r}' \Big]\phi_1(\mathbf{r},t), \tag{5}$$

$$i\frac{\partial\phi_2(\mathbf{r},t)}{\partial t} = \Big[-m_{12}\frac{\nabla^2}{2} + \frac{1}{2}m_\omega\rho^2 + g_2|\phi_2|^2 + g_{21}|\phi_1|^2 + g_{\rm dd}^{(2)} \int V_{\rm dd}(\mathbf{R})|\phi_2(\mathbf{r}',t)|^2 d\mathbf{r}' + g_{\rm dd}^{(21)} \int V_{\rm dd}(\mathbf{R})|\phi_1(\mathbf{r}',t)|^2 d\mathbf{r}' \Big]\phi_2(\mathbf{r},t), \tag{6}$$

where $\rho^2 = x^2 + y^2$, $i = \sqrt{-1}$, $m_\omega = \omega_2^2/m_{12}\omega_1^2$, $m_{12} = m_1/m_2$, $g_1 = 4\pi a_1 N_1$, $g_2 = 4\pi a_2 N_2 m_{12}$, $g_{12} = 2\pi m_1 a_{12} N_2/m_R$, $g_{21} = 2\pi m_1 a_{12} N_1/m_R$, $g_{\rm dd}^{(2)} = 3N_2 a_{\rm dd}^{(2)} m_{12}$, $g_{\rm dd}^{(1)} = 3N_1 a_{\rm dd}^{(1)}$, $g_{\rm dd}^{(12)} = 3N_2 a_{\rm dd}^{(12)} m_1/2m_R$, $g_{\rm dd}^{(21)} = 3N_1 a_{\rm dd}^{(12)} m_1/2m_R$, and ω_j is the radial frequency of the harmonic trap acting on species j. In Eqs. (5) and (6), length is expressed in units of oscillator length $l = \sqrt{\hbar/m_1\omega_1}$, energy in units of oscillator energy $\hbar\omega_1$, probability density $|\phi_j|^2$ in units of l^{-3}, and time in units of $t_0 = 1/\omega_1$.

B. Single-component BEC

The dimensionless GP equation for a single-component dipolar quasi-1D soliton is [17]

$$i\frac{\partial\phi(\mathbf{r},t)}{\partial t} = \Big[-\frac{\nabla^2}{2} + \frac{1}{2}\rho^2 + 4\pi a N|\phi(\mathbf{r},t)|^2 + 3a_{\rm dd}N \int V_{\rm dd}(\mathbf{R})|\phi(\mathbf{r}',t)|^2 d\mathbf{r}' \Big]\phi(\mathbf{r},t), \tag{7}$$

where N is the number of atoms, a is the scattering length, and $a_{\rm dd}$ is the dipolar length.

III. NUMERICAL RESULTS

The ^{164}Dy and ^{168}Er atoms have the largest magnetic moments of all the dipolar atoms used in BEC experiments. For the single-component dipolar BEC we consider ^{164}Dy atoms and for the binary dipolar BEC we consider the ^{164}Dy-^{162}Dy mixture. The magnetic moment of a single ^{164}Dy or ^{162}Dy atom is $\mu_1 = 10\mu_B$ [13] and of a ^{168}Er atom is $\mu_2 = 7\mu_B$ [14] with μ_B the Bohr magneton leading to the dipolar lengths $a_{\rm dd}(^{164}{\rm Dy}) \approx 132.7a_0$, $a_{\rm dd}(^{168}{\rm Er}) \approx 66.6a_0$, $a_{\rm dd}(^{162}{\rm Dy}) \approx 131.0a_0$, and $a_{\rm dd}(^{164}{\rm Dy}$-$^{162}{\rm Dy}) \approx 131.9a_0$, with a_0 the Bohr radius. The dipolar interaction in ^{164}Dy atoms is roughly double that in ^{168}Er atoms and about eight times larger than that in ^{52}Cr atoms with a dipolar length $a_{\rm dd} \approx 15a_0$ [15]. In both the single-component case and the binary mixture we take $l = 1$ μm. In a single-component ^{164}Dy BEC this corresponds to a radial angular trap frequency $\omega = 2\pi \times 61.6$ Hz

corresponding to $t_0 = 2.6$ ms and in a ^{168}Er BEC this corresponds to $\omega = 2\pi \times 60.2$ Hz. In the binary ^{164}Dy-^{162}Dy mixture $\omega_1 = \omega_2 = 2\pi \times 61.6$ Hz.

We solve the 3D equations (5) and (6) or Eq. (7) by the split-step Crank-Nicolson discretization scheme using both real- and imaginary-time propagation in 3D Cartesian coordinates independent of the underlying trap symmetry using a space step of 0.1–0.2 and a time step of 0.0004–0.005 [25]. The dipolar potential term is treated by Fourier transformation in momentum space using a convolution theorem in the usual fashion [26]. It was conjectured that stable quasi-1D dark solitons, with an antisymmetric wave function, are the stationary lowest axial excitation of the system [27]. They are comparable to the lowest axial excitation of a 3D harmonic oscillator with a notch. The imaginary-time simulation converges to the lowest-energy solution with the specific symmetry of the initial state. For example, in the 1D linear harmonic oscillator problem, an antisymmetric initial state leads, in the imaginary-time simulation, to the first excited state. Similarly, in the imaginary-time simulation the stationary dark-in-bright solitons can be obtained with an initial antisymmetric trial function, for example, $\phi(\mathbf{r}) \sim z \exp[-\rho^2/2 - \alpha^2 z^2/2]$, with a notch at $z = 0$ and with a small α denoting large spatial axial extension of the dark-in-bright soliton. The dark-in-bright soliton is the simplest possible soliton (after the bright soliton) in a dipolar BEC.

A. Single-component BEC

We solve Eq. (7) for different values of the scattering length a. We find that for interaction parameters of ^{164}Dy and ^{168}Er atoms the dark-in-bright and bright solitons are stable up to a critical maximum number of atoms, beyond which the system collapses [28]. In Fig. 1 we plot this critical number $N_{\rm crit}$ versus a/a_0 from numerical simulation. We find that a stable soliton is possible for $a \lesssim a_{\rm dd}$ and for a number of atoms below this critical number [17]. The critical number of atoms increases with an increase of contact repulsion as $a \to a_{\rm dd}$, which is counterintuitive. The solitons are bound by long-range dipolar interaction and an increase of contact

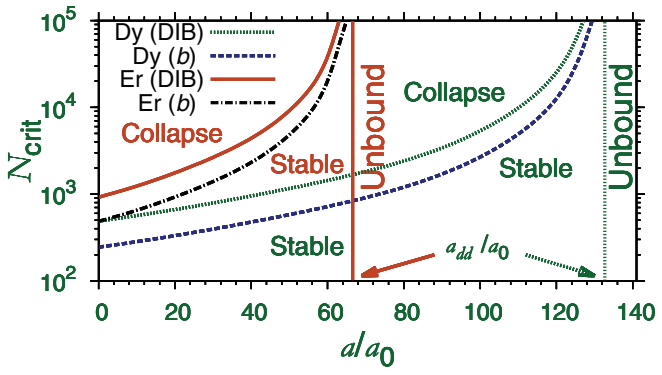

FIG. 1. (Color online) Stability phase diagram showing the critical number of atoms $N_{\rm crit}$ in a quasi-1D dipolar dark-in-bright (DIB) and bright (b) BEC soliton of ^{164}Dy or ^{168}Er atoms from numerical calculation. The system is repulsive and unbound for $a \gtrsim a_{\rm dd}$. Stable quasi-1D solitons appear for $a \lesssim a_{\rm dd}$ and the number of atoms N below the critical number $N_{\rm crit}$. The oscillator length $l = 1$ μm.

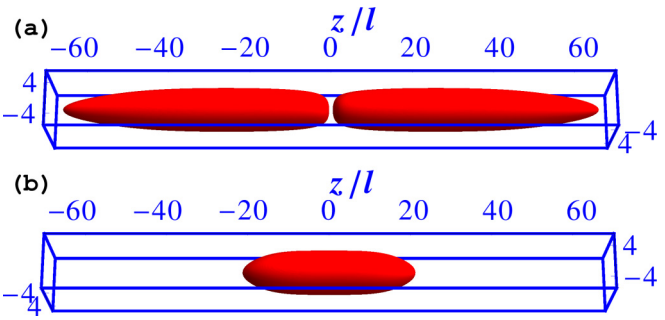

FIG. 2. (Color online) The 3D isodensity contour ($|\phi|^2$) of (a) a dark-in-bright and (b) a bright soliton of 1000 ^{164}Dy atoms with $a = 80a_0$. The dimensionless lengths x, y, and z are in units of l ($\equiv 1$ μm). The density on the contour is 10^7 atoms/cm^3 compared to the central density in the bright soliton of (b) of about 10^{12} atoms/cm^3.

repulsion gives more stability against collapse for a fixed dipolar interaction strength. In this phase diagram three regions are shown: stable, collapse, and unbound. In the unbound region ($a \gtrsim a_{\rm dd}$) contact repulsion dominates over dipolar attraction and the soliton cannot be bound. In the collapse region, the opposite happens and the soliton collapses due to an excess of dipolar attraction along the axial z direction. In the stable region there is a balance between attraction and repulsion and a stable soliton can be formed. In Figs. 2(a) and 2(b) we show the isodensity contour of a dark-in-bright and a bright soliton of 1000 ^{164}Dy atoms for $a = 80a_0$ and $l = 1$ μm. The bright soliton is much more compact with a large central density compared to the well-stretched dark-in-bright soliton with a zero central density, both free to move along

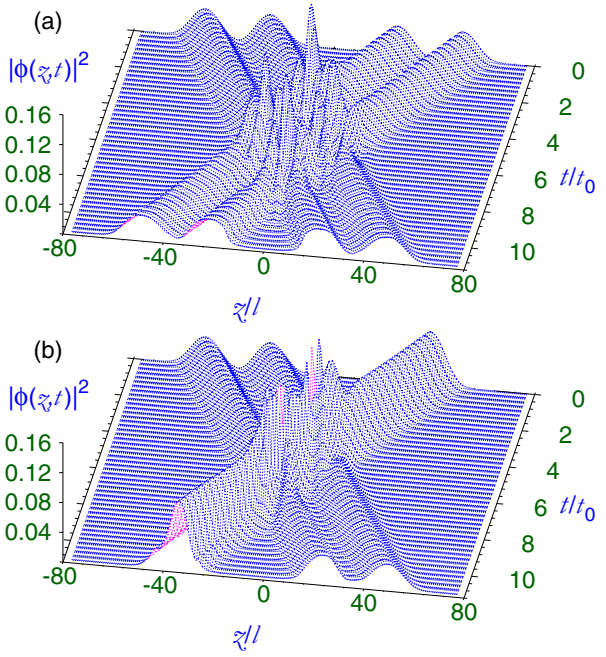

FIG. 3. (Color online) Linear axial density of (a) two colliding dark-in-bright solitons of 1000 ^{164}Dy atoms each from Fig. 2(a) and (b) the colliding dark-in-bright soliton of Fig. 2(a) and a bright soliton of 500 ^{164}Dy atoms with $a = 80a_0$.

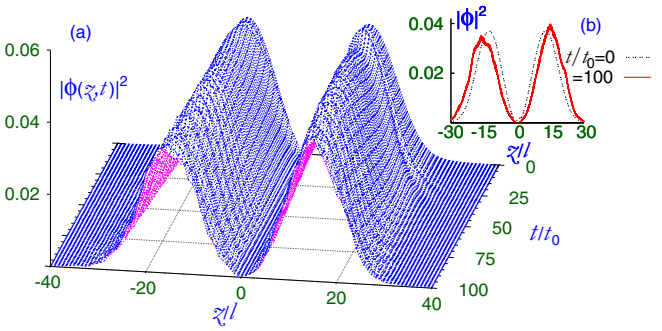

FIG. 4. (Color online) (a) Linear axial density of the dipolar dark-in-bright soliton of 1000 ^{164}Dy atoms with $a = 80a_0$ and $l = 1$ μm upon real-time propagation. The initial state has been modified to have the central zero of the dark-in-bright soliton at $z/l \approx -2$. (b) Initial ($t = 0$) and final ($t/t_0 = 100$) profiles of linear axial densities.

the axial polarization direction due to the absence of the axial trap.

Both dark-in-bright and bright solitons are unconditionally stable and last forever in real-time propagation without any visible change of shape. The dipolar attraction provides binding of the soliton and the contact repulsion reduces collapse instability. In order to have very robust solitons one should have $a_{\rm dd} \gg a \gg 0$ corresponding to more dipolar attraction over a sizable contact repulsion. For ^{164}Dy atoms with $a_{\rm dd} = 132.7a_0$, we considered $a = 80a_0$ for the illustration consistent with this inequality, which can be achieved using a Feshbach resonance [4].

To demonstrate further the robustness of the solitons we consider a head-on collision between two solitons moving along the polarization z axis in opposite directions. First, we consider the collision between two identical dark-in-bright solitons of Fig. 2(a), each of 1000 ^{164}Dy atoms. Next we consider the collision between the dark-in-bright soliton of Fig. 2(a) with a bright soliton of 500 ^{164}Dy atoms with $a = 80a_0$ and $l = 1$ μm. The constant velocity of about 2.4 mm/s of each of the colliding solitons was achieved by phase imprinting with factors of $\exp(\pm i7.5z)$ applied to the respective wave functions. In Fig. 3(a) we plot the integrated 1D density $|\phi(z,t)|^2 = \int dx\, dy |\phi(\mathbf{r},t)|^2$ of the moving dark-in-bright solitons versus z and t. The collision dynamics of a bright soliton with a dark-in-bright soliton is illustrated in Fig. 3(b) via a plot of the integrated 1D density of the two solitons. After collision, the solitons emerge in both cases without a visible change of shape demonstrating the solitonic nature. However, at much lower incident velocities the collision becomes inelastic and a distortion in the shape of the emerging solitons is found. This is expected, as only the collision between two 1D integrable solitons is truly elastic.

In the case of a normal dark soliton in a trapped BEC, long-time simulation in real-time propagation may lead to a destruction of the dark soliton by snake instability [8] and by instability against oscillation of the central zero along the axial direction [9]. We tested that the dipolar dark-in-bright soliton maintains its profile in long-time real-time propagation without snake instability (not presented in this paper). This is not surprising as a dark soliton in a trapped BEC exhibits snake instability in the presence of a strong axial trap and does not exhibit this instability in the limit of a weak axial trap. So it is reasonable that the present dark-in-bright soliton without axial trap does not exhibit snake instability. Now we test the stability of the dipolar dark-in-bright soliton when the central zero of the dark soliton is given a small displacement with respect to the center of the bright solitonic profile. For this test, we consider the dark-in-bright soliton of 1000 ^{164}Dy atoms with $a = 80a_0$ and modify the initial profile between $z/l = \pm 2$ and move the central zero of the dark-in-bright soliton from $z = 0$ to $z/l \approx -2$. With this modified initial profile of the dark-in-bright soliton we perform real-time simulation up to $t/t_0 = 100$. We find that the zero of the dark-in-bright soliton quickly moves to $z = 0$ and no unstable oscillation of this zero is noted. The dark-in-bright soliton does turn to a gray-in-bright soliton with the central notch having nonzero density. This is illustrated by a plot of linear axial density versus time in Fig. 4(a). In Fig. 4(b) we show the initial and final axial densities at $t/t_0 = 0$ and 100. As the initial state in this study is not a stationary state, oscillation in density is noted, however maintaining the central notch of the dark soliton fixed at $z = 0$, confirming the stability of the dark-in-bright soliton.

As the dark-in-bright solitons are stable and robust, they can be prepared by phase imprinting [22] a bright soliton. In experiment, a homogeneous potential generated using a far-detuned laser beam is applied on one half of the bright soliton ($z < 0$) for an interval of time so as to imprint an extra phase of π on the wave function for $z < 0$ [6]. The

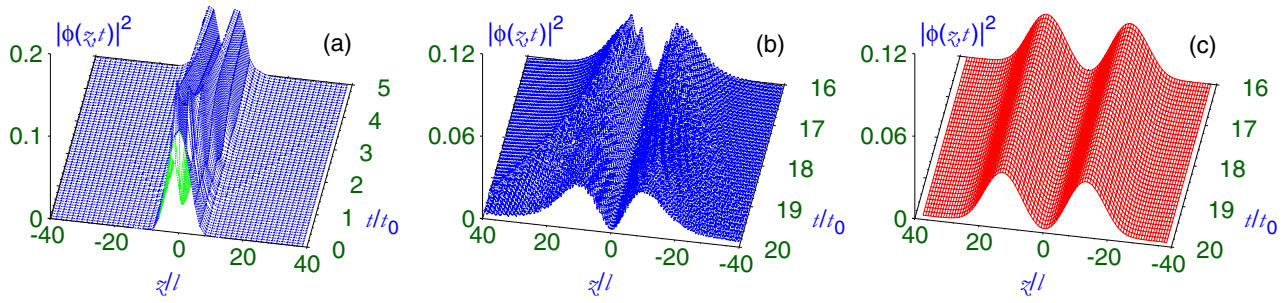

FIG. 5. (Color online) Creating a dark-in-bright soliton in a real-time simulation of a phase-imprinted bright soliton of 1000 ^{164}Dy atoms with $a = 80a_0$ and $l = 1$ μm. The linear axial density of the bright soliton (blue) is shown for (a) small ($5 > t/t_0 > 0$) and (b) large ($20 > t/t_0 > 16$) times. (c) The constant density of the stationary dark-in-bright soliton (red) of 1000 ^{164}Dy atoms obtained by an imaginary-time routine with $a = 80a_0$ and $l = 1$ μm is also shown for comparison.

thus-phase-imprinted bright soliton is propagated in real time, while it slowly transforms into a dark-in-bright soliton. The present simulation is done with no axial trap. In actual experiments a very weak axial trap can be kept during generation of the dark-in-bright soliton and eventually removed. The simulation is illustrated in Figs. 5(a) and 5(b), where we plot the linear axial density of the phase-imprinted soliton versus time at small and large times. It is demonstrated that at large times the linear density tends towards that of the stable dark-in-bright soliton with a prominent notch at the center presented in Fig. 5(c).

B. Binary BEC

The dark-in-bright solitons can also be realized in a binary dipolar BEC [29]. For illustration we consider the ^{164}Dy-^{162}Dy mixture. This is particularly interesting as Lev and his collaborators are studying this binary mixture in the laboratory at Stanford University [30]. In order to permit a large number of atoms in the solitons we consider a large value for the scattering lengths, e.g., $a(^{162}\text{Dy}) = a(^{164}\text{Dy}) = 120a_0$,(see Fig. 1). The interspecies scattering length is considered as a variable. There could be two types of new binary solitons bound by interspecies attraction [31]: (a) two coupled dark-in-bright solitons and (b) a dark-in-bright soliton coupled to a bright soliton. First we consider the stability phase plot for these two cases. In Fig. 6 we show the maximum critical number of ^{162}Dy atoms in the stable binary soliton with 1000 ^{164}Dy atoms. As the mass and dipolar lengths are almost the same for the two isotopes, the binary plot is quasisymmetric under an exchange of ^{162}Dy and ^{164}Dy atoms. The plot for 1000 ^{164}Dy atoms in the binary soliton will be practically the same as that in Fig. 6 with the role of the two isotopes interchanged. As a dark-in-bright soliton can accommodate more atoms than a bright soliton, two coupled dark-in-bright solitons can have more atoms than a dark-in-bright soliton coupled to a bright soliton.

In Fig. 7 we show the isodensity contour of a binary ^{164}Dy-^{162}Dy soliton for 1000 ^{164}Dy atoms and 3000 ^{162}Dy atoms for the interspecies scattering length $a(^{164}\text{Dy}\text{-}^{162}\text{Dy}) = 100a_0$ and intraspecies scattering lengths $a(^{164}\text{Dy}) = a(^{162}\text{Dy}) = 120a_0$. In Figs. 7(a) and 7(b) we show the profiles of the coupled dark-in-bright solitons of ^{164}Dy and ^{162}Dy atoms, respectively. In Figs. 7(c) and 7(d) we illustrate the profiles of the dark-in-bright ^{164}Dy soliton coupled to the bright ^{162}Dy soliton. The component ^{164}Dy with a smaller number of atoms has a smaller spatial extension, whereas the component ^{162}Dy with a larger number of atoms has a larger spatial extension. As the bright soliton with a large central density has a smaller spatial extension compared to a dark-in-bright soliton, the spatial extension of the bright soliton in Fig. 7(d) is much smaller than the bright-in-dark soliton in Fig. 7(b) (note the different length scales in these plots). These binary dark-in-bright solitons are found to be stable in real-time propagation upon small perturbation.

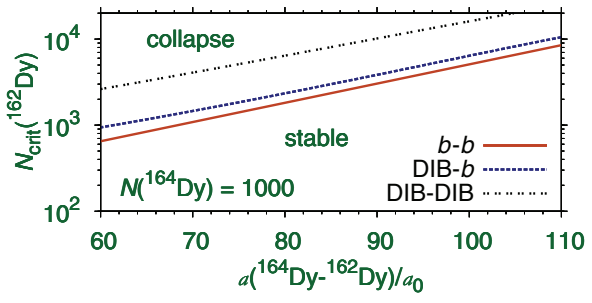

FIG. 6. (Color online) Stability phase diagram for the critical number of ^{162}Dy atoms in a binary ^{164}Dy-^{162}Dy soliton with 1000 ^{164}Dy atoms versus the interspecies scattering length with (a) two coupled bright (b-b) solitons, (b) a dark-in-bright (DIB) ^{164}Dy soliton coupled to a bright (DIB-b) ^{162}Dy soliton, and (c) two coupled DIB (DIB-DIB) solitons. The parameters are $a(^{164}\text{Dy}) = a(^{162}\text{Dy}) = 120a_0$ and $l = 1$ μm.

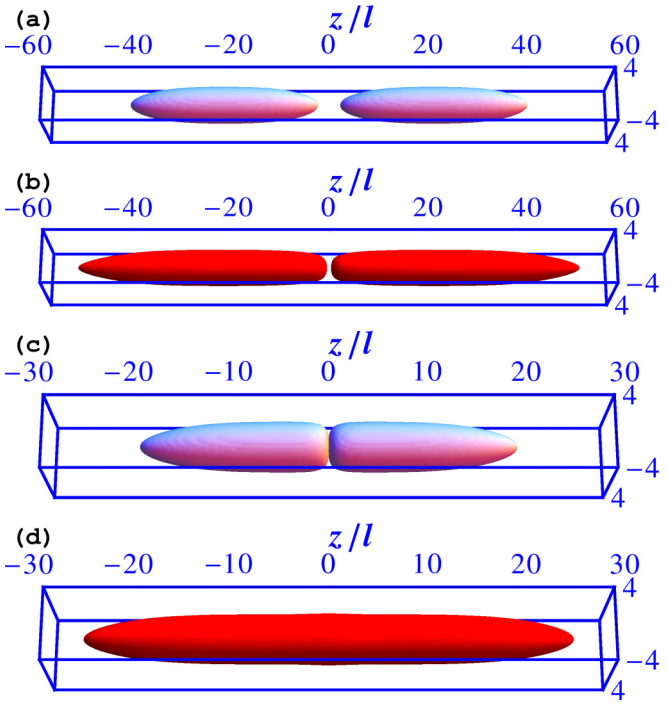

FIG. 7. (Color online) The 3D isodensity contour ($|\phi_i(\mathbf{r})|^2$) of two dark-in-bright solitons in the binary ^{164}Dy-^{162}Dy mixture: (a) ^{164}Dy and (b) ^{162}Dy profiles. Also shown is the same of a dark-in-bright and a bright soliton in the binary ^{164}Dy-^{162}Dy mixture: (c) ^{164}Dy and (d) ^{162}Dy profiles. The parameters are $a(^{164}\text{Dy}\text{-}^{162}\text{Dy}) = 100a_0$, $a(^{164}\text{Dy}) = a(^{162}\text{Dy}) = 120a_0$, $l = 1$ μm, $N(^{164}\text{Dy}) = 1000$, and $N(^{162}\text{Dy}) = 3000$. The density on the contour is 10^7 atoms/cm^3.

IV. CONCLUSION

We demonstrated the possibility of creating mobile, stable, quasi-1D, dark-in-bright solitons in dipolar BECs with a notch in the central plane capable of moving along the axial polarization direction with a constant velocity. The snake instability in trapped BEC dark solitons exists only for a weak transverse trap and disappears for a strong transverse trap [8–10]. The present solitons are stationary solutions of the mean-field GP equation and being axially free with a strong transverse trap, they do not exhibit snake instability. The head-on collision between two dark-in-bright solitons or between a bright and a dark-in-bright soliton with a relative velocity of about 5 mm/s is quasielastic with the solitons passing through each other with practically no deformation.

A possible way of preparing the dark-in-bright soliton by phase imprinting was illustrated. In addition to an isolated dark-in-bright soliton, we also demonstrated the viability of preparing these solitons in a binary dipolar BEC as two coupled dark-in-bright solitons or as a bright soliton coupled to a dark-in-bright soliton. The numerical simulation was done by explicitly solving the 3D GP equation with realistic values of contact and dipolar interactions of ^{164}Dy and ^{162}Dy atoms. The results and conclusions of the present paper can be tested in experiments with present-day know-how and technology and should lead to interesting future investigations.

ACKNOWLEDGMENTS

We thank FAPESP and CNPq (Brazil) for partial support.

[1] Y. S. Kivshar and B. A. Malomed, Rev. Mod. Phys. **61**, 763 (1989); F. K. Abdullaev, A. Gammal, A. M. Kamchatnov, and L. Tomio, Int. J. Mod. Phys. B **19**, 3415 (2005).

[2] K. E. Strecker, G. B. Partridge, A. G. Truscott, and R. G. Hulet, Nature (London) **417**, 150 (2002); L. Khaykovich, F. Schreck, G. Ferrari, T. Bourdel, J. Cubizolles, L. D. Carr, Y. Castin, and C. Salomon, Science **296**, 1290 (2002).

[3] S. L. Cornish, S. T. Thompson, and C. E. Wieman, Phys. Rev. Lett. **96**, 170401 (2006).

[4] S. Inouye, M. R. Andrews, J. Stenger, H.-J. Miesner, D. M. Stamper-Kurn, and W. Ketterle, Nature (London) **392**, 151 (1998).

[5] V. M. Pérez-García, H. Michinel, and H. Herrero, Phys. Rev. A **57**, 3837 (1998).

[6] S. Burger, K. Bongs, S. Dettmer, W. Ertmer, K. Sengstock, A. Sanpera, G. V. Shlyapnikov, and M. Lewenstein, Phys. Rev. Lett. **83**, 5198 (1999).

[7] J. Denschlag, J. E. Simsarian, D. L. Feder, C. W. Clark, L. A. Collins, J. Cubizolles, L. Deng, E. W. Hagley, K. Helmerson, W. P. Reinhardt, S. L. Rolston, B. I. Schneider, and W. D. Phillips, Science **287**, 97 (2000).

[8] D. J. Frantzeskakis, J. Phys. A **43**, 213001 (2010).

[9] Th. Busch and J. R. Anglin, Phys. Rev. Lett. **84**, 2298 (2000).

[10] A. Muryshev, G. V. Shlyapnikov, W. Ertmer, K. Sengstock, and M. Lewenstein, Phys. Rev. Lett. **89**, 110401 (2002).

[11] B. P. Anderson, P. C. Haljan, C. A. Regal, D. L. Feder, L. A. Collins, C. W. Clark, and E. A. Cornell, Phys. Rev. Lett. **86**, 2926 (2001).

[12] M. Lu, S. H. Youn, and B. L. Lev, Phys. Rev. Lett. **104**, 063001 (2010); J. J. McClelland and J. L. Hanssen, *ibid.* **96**, 143005 (2006); S. H. Youn, M. W. Lu, U. Ray, and B. V. Lev, Phys. Rev. A **82**, 043425 (2010).

[13] M. Lu, N. Q. Burdick, S. H. Youn, and B. L. Lev, Phys. Rev. Lett. **107**, 190401 (2011).

[14] K. Aikawa, A. Frisch, M. Mark, S. Baier, A. Rietzler, R. Grimm, and F. Ferlaino, Phys. Rev. Lett. **108**, 210401 (2012).

[15] T. Lahaye, T. Koch, B. Fröhlich, M. Fattori, J. Metz, A. Griesmaier, S. Giovanazzi, and T. Pfau, Nature (London) **448**, 672 (2007); A. Griesmaier, J. Stuhler, T. Koch, M. Fattori, T. Pfau, and S. Giovanazzi, Phys. Rev. Lett. **97**, 250402 (2006).

[16] J. Stuhler, A. Griesmaier, T. Koch, M. Fattori, T. Pfau, S. Giovanazzi, P. Pedri, and L. Santos, Phys. Rev. Lett. **95**, 150406 (2005); K. Goral, K. Rzazewski, and T. Pfau, Phys. Rev. A **61**, 051601 (2000); T. Koch, T. Lahaye, J. Metz, B. Fröhlich, A. Griesmaier, and T. Pfau, Nat. Phys. **4**, 218 (2008); T. Lahaye, C. Menotti, L. Santos, M. Lewenstein, and T. Pfau, Rep. Prog. Phys. **72**, 126401 (2009).

[17] L. E. Young-S., P. Muruganandam, and S. K. Adhikari, J. Phys. B **44**, 101001 (2011).

[18] R. Nath, P. Pedri, and L. Santos, Phys. Rev. Lett. **102**, 050401 (2009); P. Pedri and L. Santos, *ibid.* **95**, 200404 (2005); I. I. Tikhonenkov, B. A. Malomed, and A. Vardi, *ibid.* **100**, 090406 (2008); P. Köberle, D. Zajec, G. Wunner, and B. A. Malomed, Phys. Rev. A **85**, 023630 (2012); R. Eichler, D. Zajec, P. Köberle, J. Main, and G. Wunner, *ibid.* **86**, 053611 (2012); R. Eichler, J. Main, and G. Wunner, *ibid.* **83**, 053604 (2011); A.-X. Zhang and J.-K. Xue, *ibid.* **82**, 013606 (2010); V. M. Lashkin, *ibid.* **75**, 043607 (2007).

[19] S. K. Adhikari and P. Muruganandam, J. Phys. B **45**, 045301 (2012); I. Tikhonenkov, B. A. Malomed, and A. Vardi, Phys. Rev. A **78**, 043614 (2008).

[20] R. Nath, P. Pedri, and L. Santos, Phys. Rev. Lett. **101**, 210402 (2008).

[21] S. K. Adhikari and P. Muruganandam, Phys. Lett. A **376**, 2200 (2012).

[22] L. Dobrek, M. Gajda, M. Lewenstein, K. Sengstock, G. Birkl, and W. Ertmer, Phys. Rev. A **60**, R3381 (1999).

[23] L. E. Young-S. and S. K. Adhikari, Phys. Rev. A **86**, 063611 (2012); **87**, 013618 (2013).

[24] S. K. Adhikari, Phys. Rev. A **88**, 043603 (2013).

[25] P. Muruganandam and S. K. Adhikari, Comput. Phys. Commun. **180**, 1888 (2009); D. Vudragovic, I. Vidanovic, A. Balaz, P. Muruganandam, and S. K. Adhikari, *ibid.* **183**, 2021 (2012); S. K. Adhikari and P. Muruganandam, J. Phys. B **35**, 2831 (2002).

[26] K. Goral and L. Santos, Phys. Rev. A **66**, 023613 (2002); S. Yi and L. You, *ibid.* **63**, 053607 (2001).

[27] S. K. Adhikari, J. Low Temp. Phys. **143**, 267 (2006).

[28] S. Ronen, D. C. E. Bortolotti, and J. L. Bohn, Phys. Rev. Lett. **98**, 030406 (2007).

[29] R. M. Wilson, C. Ticknor, J. L. Bohn, and E. Timmermans, Phys. Rev. A **86**, 033606 (2012); H. Saito, Y. Kawaguchi, and M. Ueda, Phys. Rev. Lett. **102**, 230403 (2009).

[30] B. L. Lev (private communication).

[31] S. K. Adhikari, Phys. Lett. A **346**, 179 (2005).